

# Correction of LIF temperature measurements for laser absorption and fluorescence trapping in a flame

## Application to the thermal perturbation study induced by a sampling probe

P. Desgroux\*, L. Gasnot, J.F. Pauwels, L.R. Sochet

Laboratoire de Cinétique et Chimie de la Combustion, URA CNRS 876, Université des Sciences et Technologies de Lille, F-59655 Villeneuve d'Ascq Cedex, France  
(Fax: + 33/20436977)

Received: 29 July 1994 / Accepted: 25 January 1995

**Abstract.** A computational method is described in order to correct OH LIF temperature measurements for absorption of laser energy and trapping of fluorescence. Calculations are performed in a large range of flame conditions and can be used as a correction data base both in case of (0–0) and (1–0) excitations. Comparison of corrected temperatures profiles obtained in a 40 Torr methanol/air flame, for both kinds of Laser-Induced Fluorescence (LIF) excitations shows a very good agreement. This method is applied to measure the temperature profile of a methanol flame perturbed by a sampling probe. The LIF collection volume is located at the actual probe sampled volume using an experimental procedure already described. Spatial resolution and sensitivity of temperature measurements are sufficiently efficient to highlight, for the first time by LIF, an indubitable cooling effect due to the probe presence that induces important OH profile change. According to flame chemical modelling, it is shown that both effects are strongly correlated.

**PACS:** 33.00; 82.20. Wt

An accurate temperature measurement in flames is absolutely required because of the high sensitivity of flame kinetics to the temperature. In most cases, the flame temperature profile is determined by using intrusive coated thermocouples. Temperature corrections for conduction, radiation losses or catalytic effects are needed. Difficulty of temperature measurement increases with the use of probe sampling techniques. Indeed, a major concern of sampling techniques is the proper handling of the effective probe sampling location which is generally admitted to be a few orifice diameters in front of the cone tip [1]. Thermocouple is placed at the presumed location of the sampled volume and temperatures are found very sensitive to probe position [2]. Thus, the inaccuracy of probe volume

location can strongly affect the knowledge of the actual flame temperature and therefore flame kinetics understanding.

Temperature determination using Laser-Induced Fluorescence (LIF) is generally admitted to be more accurate than by thermocouples. Measurements are usually performed on the hydroxyl radical. But relatively high concentration of this radical contributes to absorb the incident laser energy and the fluorescence emission. By exciting OH (1–0) vibronic band, trapping/absorption effects were thought to be overcome but this assumption would deserve some investigations. Moreover temperature determination from (1–0) excitation must take into account Vibrational Energy Transfer (VET) and quantum yields dependence with rotational number [3, 4]. With (0–0) excitation, these problems are not so crucial but trapping/absorption effects are more important. Only one group reports compensation of these effects by selecting a judicious LIF collection volume location [3, 5].

This work is devoted to improve flame temperature measurements by LIF, particularly in the vicinity of a sampling probe. First, a method that takes into account both trapping and absorption effects for OH (0–0) and (1–0) excitations is developed. Attenuation of LIF intensities is calculated according to spectroscopic analysis and absorption coefficients. An automatic correction of LIF spectra is generated by a computer code and corrections are calculated for many flame conditions. Comparison of corrected temperatures, obtained for both kinds of excitations, are performed in a 40 torr methanol/air flame. Then, we test our temperature measurements in the vicinity of a sampling probe, in view of further coupling of laser and probe sampling techniques. Measurements are performed in the previous flame in the presence or not of the sampling probe. Coincidence of LIF and probe sampling volumes has been obtained according to a method demonstrated in a previous work [6]. Briefly, it consists to compare OH profiles obtained either by Electron Spin Resonance (ESR) or by LIF. By moving the extraction cone relatively to the LIF collection volume, coincidence in shape, location and absolute value between both OH

\* To whom all correspondence should be addressed

profiles is obtained for a given laser/probe distance. Therefore, hydroxyl concentrations, spatially averaged over both sampling volumes (ESR and LIF) are nearly identical for the selected probe/laser distance. In these conditions, OH LIF measurements are performed within the effective probe sampling volume. This procedure is extended to (i) highlight by LIF the cooling effect induced by a sampling probe and (ii) determine the actual temperature of the probe sampled volume. Correlation between the observed thermal perturbation and OH profile change, due to the probe introduction, is then tested by comparison with OH modelling.

## 1 Experimental

### 1.1 Arrangement

The experimental arrangement, shown in Fig. 1, consists in the low-pressure burner, the laser diagnostic system and the ESR detection system. It has been described previously [2, 6]. Measurements have been performed in a 40 Torr premixed methanol/air flame (equivalence ratio: 1.08; total flow rate: 5.9 l/min) stabilized on a 6 cm diameter burner. Laser position is kept constant during the experiments. Burner is translated vertically to obtain OH species and temperature evolutions through the flame reaction zone. The low-pressure flame chamber is equipped with a sampling quartz probe (orifice diameter of 0.12 mm) connected with the ESR cavity [2]. Disconnected from the ESR extraction system, the probe can be translated along the vertical axis of the burner in order to change its location relatively to the LIF collection volume. In this work, laser/probe distance is  $< 0.3$  mm.

Laser system consists of a frequency doubled Quantel Nd: YAG laser pumping a dye laser. Laser pulse duration is 7 ns and laser bandwidth is  $0.1 \text{ cm}^{-1}$ . By using different dyes mixtures (rhodamine 590 or a mixture of rhodamine 640 and DCM), the (1-0) and (0-0) OH vibrational bands have been successively excited around 280 and 307 nm respectively. The 12 mJ laser beam is attenuated by using reflexion on two beamsplitters and neutral densities. The resulting low laser energy (a few  $\mu\text{J}$  per pulse) is required to insure linearity of LIF signal with laser power. Laser beam is focused by a 500 mm focal length lens. Laser energy fluctuations are monitored by a postflame photodiode which also measures absorption of the laser beam over the 6 cm path length through the flame. Fluorescence signal is collected at  $f/4$  by a two-lens system and focused onto the entrance slit (0.4 mm width, 2 mm height) of a 0.25 m monochromator. The entrance slit is parallel to the laser axis and the output slit is modified to provide a wide bandpass adapted to the fluorescence band under investigation. For laser absorption measurements, the focused lens is replaced by a 0.8 mm diameter pinhole and the laser energy is monitored by a photodiode located before the burner chamber. Fluorescence and laser intensity signals are simultaneously time-resolved and stored by a Tektronix DSA 602A Digitizing Signal Analyser (1 GHz bandwidth and 1 GS/s sampling rate per channel) recorded to a microcomputer.

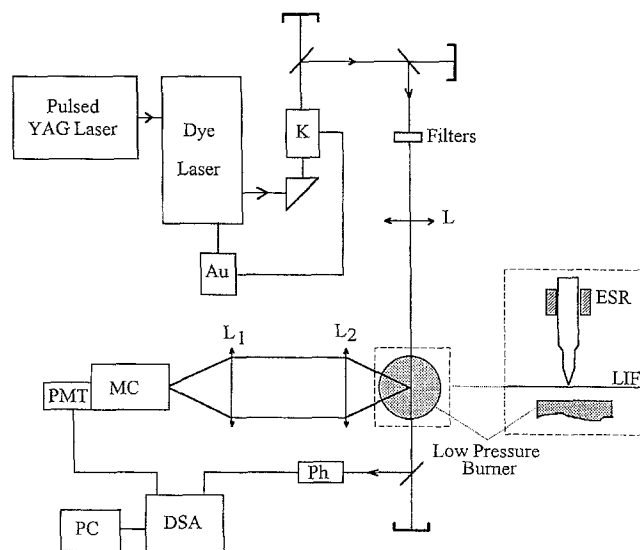


**Fig. 1.** Experimental arrangement for the LIF measurements. K: second harmonic generator; Au: automatic tracking of K orientation with wavelength emission of the dye laser; L: focused lens;  $L_1$ ,  $L_2$ , collecting lenses; Ph: postflame photodiode; MC: monochromator; PMT: photomultiplier; DSA: Digitizing Signal Analyser; ESR: Electron Spin Resonance cavity

### 1.2 Laser diagnostic method

In the linear regime of fluorescence [7], the broadband fluorescence signal SF obtained when exciting from level  $i$  in the ground state to level  $j$  in the excited state, and normalized by the laser intensity  $U$ , is given by the relation

$$\text{SF}/U = G(A/A + Q) B_{ij} N_i, \quad (1)$$

where  $G$  is a constant depending on collection efficiency.  $A$  and  $B_{ij}$  are the Einstein coefficient for spontaneous emission and absorption respectively.  $A = \sum_l A_{lj}$ , where  $l$  denotes rotational levels of lower electronic state towards which allowed rotational transitions occur.  $Q$  is the total collisional quenching rate and  $(A/A + Q)$  is the fluorescence quantum yield.  $N_i$  is the population in level  $i$ .

Relative OH number density profiles are obtained by collecting fluorescence intensity upon excitation of the  $Q_1(6)$  transition of the (0-0) band. LIF intensity is averaged over 128 laser shots and corrected for laser intensity fluctuations. Correction for collection solid angle occlusion, which appears as the laser/burner distance decreases, is performed. Quenching variation with height above the burner is found negligible. Absolute scale of OH number density is determined by performing the laser absorption technique on the  $Q_1(6)$  transition [8]. Final step in determining absolute OH concentration is obtained through the Boltzmann distribution law to account for the Boltzmann fraction of the absorbing level at the local temperature.

Rotational temperature is deduced from the slope of the Boltzmann plot:  $\ln(N_i/g_i)$  vs the rotational energy of level  $i$ , where  $g_i$  is the level degeneracy. Variation of

rotational energy on a large range is obtained by exciting a great number of isolated rotational levels in the OH ground electronic state. (0–0) and (1–0) vibrational bands of OH ( $A^2\Sigma^+ \leftarrow X^2\Pi$ ) are investigated using  $R_1(4, 5, 6, 9, 13)$  and  $R_2(4, 5, 7, 9, 10, 13, 14)$  transitions for (0–0) excitation and  $R_1(7, 8, 9, 10, 12, 14)$  and  $R_2(1, 2, 5, 8, 10, 11, 13)$  transitions for (1–0) excitation. Some specific problems occur with each kind of vibrational excitation. For example, in case of (1–0) excitation, rotational and Vibrational Energy Transfers (VET) from  $v' = 1$  to  $v' = 0$  contribute to a greater dependence of quantum yield with rotational energy level [4, 9–11]. This dependence is reduced by collecting the fluorescence in the entire (0–0) and (1–1) bands [12]. From the time-resolved fluorescence signals, fluorescence de-excitation rates have been measured in our flame on a large range of excited-state rotational levels and a 5% quenching decrease has been found with increasing investigated rotational energies. To minimize this effect of rotational-level-dependent quantum yields, fluorescence intensity is sampled promptly after laser pulse [3, 5] with a 1 GHz sampling rate. Long duration of OH fluorescence pulses in low-pressure flames enables this time resolution. In the case of (0–0) excitation, the more crucial problem is the attenuation of fluorescence intensities due to absorption of laser energy and trapping of fluorescence.

## 2 Calculation of temperature corrections

Attenuation of the LIF signal due to laser energy absorption has been taken into account in some papers, through computational correcting procedures [13], using a post-flame photodiode [3, 5, 14] or has been used as a local absorption measurement technique [15]. Usually, trapping of fluorescence is neglected, which can lead to substantial errors in temperature measurement especially in the case of (0–0) excitation. In [3, 5], effects of trapping and absorption were approximately compensated by locating the LIF collection volume far from the burner center. This experimental method implies that the correction is independent of height above the burner and requires adaptation with flame parameters changes (mixture, pressure, temperature, etc). The theoretical method, described in this part, corrects fluorescence intensities for both laser absorption and trapping. Optical thin limit is used for simplification.

When the laser line is tuned on a selected ( $i \rightarrow j$ ) absorption transition of a molecule, the spectral laser energy attenuation, through a uniform medium of length  $x$ , is calculated according to the Lambert-Beer exponential decay:

$$U(x) = U(0) \exp(-k_{ij}x), \quad (2)$$

where  $U(0)$  is the laser intensity before the absorbing medium,  $U(x)$  is the laser intensity after the optical path length  $x$  in the flame and  $k_{ij}$  is the absorption coefficient at the laser wavelength  $\lambda_{ij}$ . In the case of LIF narrowband detection at the excitation wavelength, attenuation of fluorescence signal due to trapping can be calculated according to similar process and using the same absorption coefficient. Then the narrowband fluorescence signal

$SF_{\text{narr},ij}$  measured by the detector is given by the expression:

$$\begin{aligned} SF_{\text{narr},ij} &= SF_{ij} \exp(-k_{ij}L) \\ &= G \frac{A_{ij} \exp(-k_{ij}L)}{A_{ij} + Q} B_{ij} N_i U(x), \end{aligned} \quad (3)$$

where  $SF_{ij}$  is the narrowband fluorescence signal that would be measured without trapping, available at the collection volume location, and  $L$  is the trapping path length. In the case of broadband detection, each radiative transition of the fluorescence spectrum is attenuated according to its own absorption coefficient  $k_{ij}$ . Subscripts  $l, j$  specify rotational transitions  $j \rightarrow l$  taken into account in the broadband detection upon preliminary  $i \rightarrow j$  excitation. The measured fluorescence signal  $SF_{\text{broad},ij}$  is given by:

$$\begin{aligned} SF_{\text{broad},ij} &= \sum_l SF_{lj} \exp(-k_{lj}L) \\ &= G \frac{\sum_l A_{lj} \exp(-k_{lj}L)}{\sum_l A_{lj} + Q} B_{ij} N_i U(x). \end{aligned} \quad (4)$$

$SF_{\text{broad},ij}$  is normalized by the laser energy  $U(\text{Ph})$ , measured by a photodiode, in order to compensate for laser energy fluctuations.  $U(\text{Ph})$  depends on the photodiode location relative to the LIF collection volume. The broadband fluorescence signal, available at the collection volume location which has to be taken into account is

$$\sum_l SF_{lj} = G \frac{\sum_l A_{lj}}{\sum_l A_{lj} + Q} B_{ij} N_i U(x),$$

where  $U(x)$  is the available laser energy.

Finally, laser absorption and trapping are taken into account by applying, to the measured normalized broadband fluorescence signal  $SF_{\text{broad},ij}/U(\text{Ph})$ , the following correction:

$$\text{Corr}_{ij} = \frac{\sum_l SF_{lj}/U(x)}{SF_{\text{broad},ij}/U(\text{Ph})} = \frac{\sum_l A_{lj}}{\sum_l A_{lj} \exp(-k_{lj}L)} \frac{U(\text{Ph})}{U(x)}. \quad (5)$$

This correction is calculated using an iterative computer algorithm (Fig. 2). OH spectroscopic data are obtained from tabulated transition probabilities [16]. OH population in the  $i$  level, at the distance  $d$  above the burner, is deduced from a preliminary measurement of the absolute population in the  $J'' = 6.5$  rotational level (measured by laser absorption) and from the Boltzmann law. For a selected ( $i \rightarrow j$ ) transition, absorption coefficients  $k_{ij}$  and  $k_{lj}$  are deduced from the peak absorption coefficient  $k_{ij}^o$  [8] of a purely Doppler broadened line after compensation for laser bandwidth [13].  $k_{ij}^o$  is a function of the rotational line absorption oscillator strength and of the population  $N_i$  of hydroxyl radical. Normalized fluorescence intensities are then corrected using (5). A subroutine calculates the corrected temperature using the Boltzmann-plot technique. Computational procedure converges after  $M$  iterations.

In fact, one difficulty of the correction method lies in the selection of the involved rotational level  $l$  and their

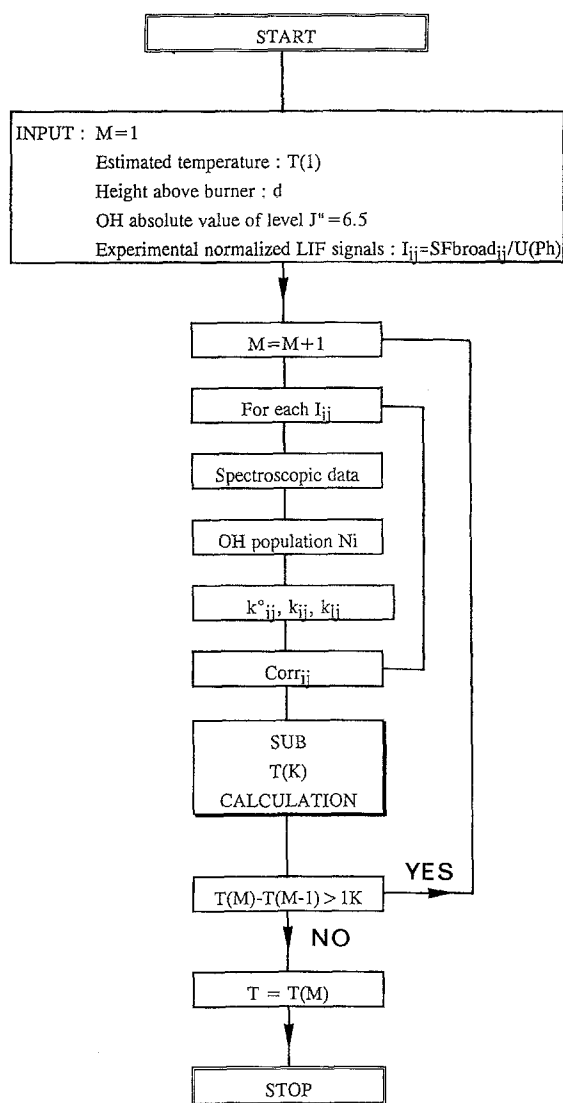


Fig. 2. Flowchart describing the iterative computer algorithm used for temperature correction

population determination. In case of (0-0) excitation,  $l$  levels are easily determined according to spectroscopic selection rules which is not true in case of (1-0) excitation, where VET induces population redistribution. In that case, trapping in (1-1) band is evidently negligible but should be taken into account in the (0-0) band according to the vibrational population value in  $v' = 0$ . In an attempt to determine this population, the ratio of (0-0) to (1-1) broadband fluorescence intensities has been measured in our flame. It decreases from 20 to 12% with increasing excited rotational level in  $v' = 1$ . From the mean ratio and considering a mean rotational transition probability in each vibrational band, the vibrational population, transferred by VET in  $v' = 0$ , is estimated to be about 8% of the excited population in  $v' = 1$ . This low value of excited population in  $v' = 0$ , following (1-0) excitation, implies that total fluorescence intensities, collected on both (0-0) and (1-1) bands, are little affected by variation of (0-0) fluorescence attenuation with rotational

number, so as vibrational transferred population distribution in  $v' = 0$  is little dependent on the originally excited rotational level in  $v' = 1$  [9, 10, 12]. In our flame, the trapping effect upon (1-0) excitation is then negligible and solely the laser absorption in (1-0) is considered. Typically, in the burnt gases of our flame, where the OH concentration is  $0.2 \times 10^{16} \text{ cm}^{-3}$ , correction reaches 40 K in the case of (0-0) excitation and 10 K upon (1-0) excitation. Corrections are of the order of the error limit of LIF method and a systematic error would be introduced by neglecting them. Furthermore, in case of higher OH density, not corrected temperatures could modify the interpretation of flame kinetics.

In an attempt to provide more general results, corrections have been carried out for several absorbing conditions within premixed flat flames, by using the inverse computational procedure. The corrected temperature is given by  $T_{\text{corrected}} = T_{\text{measured}} + \Delta T_{\text{total}}$ .  $T_{\text{measured}}$  is the temperature obtained from the not-corrected Boltzmann plot;  $\Delta T_{\text{total}}$  is the total temperature correction taking into account both trapping ( $\Delta T_{\text{trapping}}$ ) and laser absorption ( $\Delta T_{\text{abs}}$ ). Within the flame temperature range, the lower rotational levels absorb more than the higher levels because low levels are higher populated and also have larger oscillator strengths. With increased absorption of the fluorescence by lower rotational levels, the apparent temperature deduced from Boltzmann plot becomes too high. Therefore  $\Delta T_{\text{trapping}}$  is  $< 0$ . In like manner, absorption variation of the incident laser energy with involved rotational levels induces Boltzmann slope change, whose orientation depends on the photodiode location relatively to the LIF collection volume. In case of a photodiode located before the burner,  $\Delta T_{\text{abs}}$  is  $< 0$ . In the case of postflame photodiode monitoring,  $\Delta T_{\text{abs}}$  is  $> 0$ . It is clear that the use of a postflame photodiode reduces the total required correction. Simulation is carried out considering a LIF collection volume at the burner center, a burner diameter of 6 cm, and a postflame photodiode. Calculation does not require the flame composition.

Absolute values of total temperature corrections are reported in Fig. 3 for both kinds of excitation and for several flame temperatures, within an OH concentration range compatible with the optical thin assumption. Optical thin limit implies that  $\ln(\text{Corr}_{ij})$ , involved in the Boltzmann plot, is proportional to the OH concentration (or burner diameter) through the  $k_{ij}$  term. It explains the linear behaviour of temperature correction with OH concentration. This linearity is no more valid for higher optical depths. In the case of (0-0) excitation (lines), the ratio  $\Delta T_{\text{trapping}}/\Delta T_{\text{abs}}$  is found to increase from 1.5 to 2 as the temperature varies from 1200 to 2200 K. This temperature dependence limits the experimental expedient such as the use of a judicious optical arrangement to compensate trapping/absorption effects [3, 5]. (1-0) excitation appears more satisfying according to the evidently lower temperature corrections, although they are not negligible as usually assumed. Nevertheless, application of (1-0) excitation in unknown flames requires a preliminary study in order to (1) assure that (0-0) trapping is negligible, as assumed in our computation and (2) correct LIF intensities from quantum yields variations in case of atmospheric or high pressure flames. If not performed,

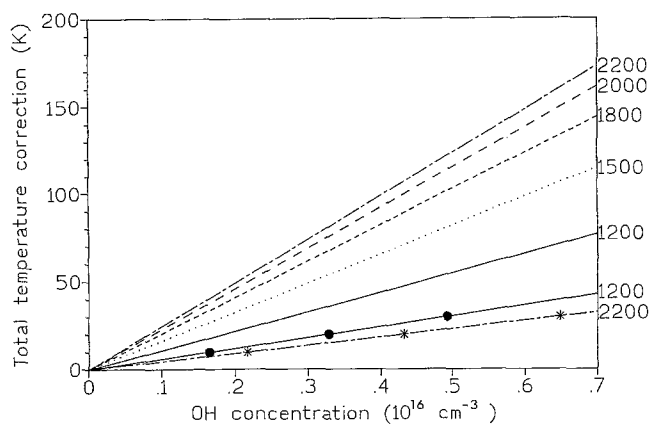


**Fig. 3.** Computed temperature corrections (absolute value) as a function of OH concentration obtained for different flame temperatures. Lines are corrections following (0–0) excitation, symbols for (1–0) excitation. Optical thin limit is used. Fluorescence signals are normalized by laser energy measured after absorption through the 6 cm diameter burner

temperature determination from (0–0) excitation is more direct and accurate, although the temperature correction is important. In that case, Fig. 3 can be useful for temperature correction data base, in a large range of flame conditions, keeping in mind that the optical thin limit is needed and the pressure broadening is not taken into account. For example, in a 2 cm diameter  $\text{CH}_4/\text{air}$  flat flame stabilized at a few bars, OH concentration reaches  $1.5 \times 10^{16} \text{ cm}^{-3}$  [17] and temperature determination error would be more than 100 K in the case of (0–0) excitation and 25 K in the case of (1–0) excitation.

### 3 Application to the flame thermal perturbation induced by a sampling probe

Most of flame structure analyses are performed using probe sampling techniques and accurate temperature determination of the actual probe sampled volume is still a challenge. Recently, comparison of OH gradients positions obtained either by LIF or probe sampling technique (ESR) was demonstrated as an excellent check to take into account the probe influence and to coincide the LIF collection volume with the effective probe sampled volume [6]. In order to extend the probe perturbation study to its thermal effects, an accurate temperature measurement is required. The corrected LIF method, described in part 2, is applied with this end of view. Measurements are performed in a 40 Torr methanol/air flame without and with the presence of the probe. Laser/probe distance ( $< 300 \mu\text{m}$ ) has been adjusted according to the experimental method previously described [6].

#### 3.1 Temperature profiles

Temperature profiles are shown in Fig. 4. Temperature is measured by using an uncoated chromel–alumel ther-

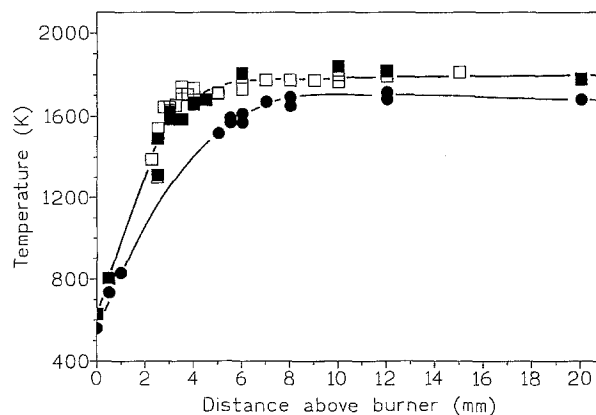


**Fig. 4.** Comparison of temperature profiles without (*squares*) and with (*circles*) the probe in the 40 Torr  $\text{CH}_3\text{OH}/\text{Air}$  flame. *Open* and *closed symbols* are temperature measurements obtained by following, respectively, (1–0) and (0–0) excitation. Probe/laser distance is  $< 300 \mu\text{m}$ . Burner surface temperature is measured by a thermocouple

mocouple ( $100 \mu\text{m}$  diameter wires), up to 1 mm from the burner surface, in the preheat zone of the flame where no radiation correction is necessary. The LIF technique is performed in the flame zone and in the burnt gases. Excitation of a large range of OH rotational transitions and averaging over a great number of laser shots by selecting a slow wavelength scanning rate, lead to a very good reproducibility of temperature determination. Temperature corrections, which reach 40 K in the burnt gases upon (0–0) excitation, are important in comparison with the statistical error which is usually less than 30 K according to Boltzmann plot accuracy. Corrected temperatures, measured either from (0–0) or (1–0) excitation, are in very good agreement. It suggests that (1) the quantum yield effect is well taken into account in both kinds of excitation by selecting appropriate bandpass detector and laser-detector timing and (2) the absorption/trapping correction method is performant.

An attempt of detecting thermal perturbation was performed by Smith and Chandler [18] by measuring LIF CN rotational temperature in presence or not of a probe. CN measurements were performed in the reaction zone where a sharp temperature gradient is present, involving spatial resolution problems. Reproducibility of temperature measurements was within 70 K and probably insufficient to detect systematic cooling effect even it was presumed. On the contrary, cooling effect has been already demonstrated by using a thermocouple [1, 2] but ambiguity concerning probe volume location always occurred.

In our case, an indubitable thermal perturbation induced by the probe is pointed out at the actual probe volume location. In presence of the probe, the temperature gradient is less pronounced in the reaction zone while a 100 K cooling effect is found in the burnt gases. To our knowledge, this perturbation is highlighted for the first time by LIF.

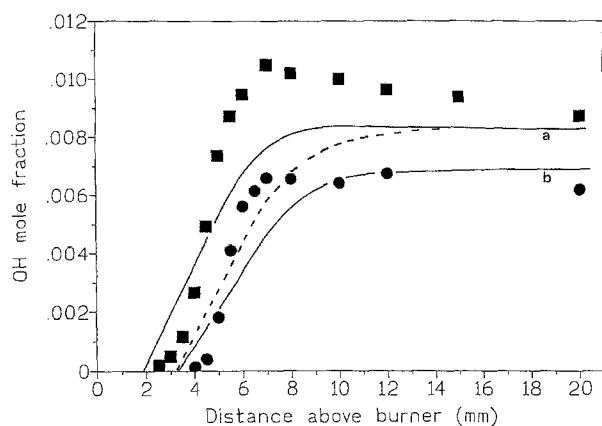


**Fig. 5.** OH mole fraction profiles, obtained by LIF, in a 40 torr  $\text{CH}_3\text{OH}/\text{Air}$  flame. Absolute calibration was obtained from laser absorption. *Squares*: profile without probe; *Circles*: profile with probe. *Solid lines* are computed OH mole fraction profiles, *a*: without the probe and *b*: with the probe. The *dashed line* is the computed OH profile calculated from the not-corrected temperature profile (photodiode before the burner)

### 3.2 OH profiles

Figure 5 shows OH mole fraction profiles obtained by LIF (symbols) without and with the presence of the probe. In the burnt gases, at 12 mm above the burner surface, absolute OH population of rotational level  $J'' = 6.5$ , measured by laser-absorption, is  $N_J = (5.4 \pm 1.5) 10^{13} \text{ cm}^{-3}$ . The probe presence induces a large downstream shift of 800  $\mu\text{m}$  of OH profile corresponding approximately to 7 times the probe orifice diameter and a 30% decrease of OH mole fraction in the burnt gases, where OH reaches its equilibrium value. Expected in a 80 Torr methanol/air flame [6], such systematic decrease in flame burnt gases was not related in the literature. The reason is probably due to the coupling of different experimental techniques used to compare species profiles without or with the probe. Stepowski et al. [19] compared OH profiles obtained by LIF, MBMS and laser-absorption. They used an arbitrary calibration in the burnt gases. Cattolica et al. [20] compared OH profiles obtained by laser-absorption and Molecular Beam Mass Spectrometry (MBMS). MBMS OH profile was calibrated assuming the partial equilibrium. The comparison of absolute  $[\text{OH}]$  profiles showed a good agreement in both OH peak value and decay rate.

In our case a direct comparison of OH profiles obtained with the same LIF technique, with and without the probe, is available and probably more accurate. In fact the highly reactive hydroxyl radical is particularly sensitive to flame temperature variations [2]. As our OH LIF measurements are performed at the location of the probe sampled volume, where an important cooling effect has been detected, thermal perturbation is probably the main reason of OH concentration change in the burnt gases.

### 3.3 Correlation between cooling effect and OH profile change

The accuracy of LIF temperature measurements allows to correlate temperature and OH profiles changes observed by introducing the quartz probe in the flame. An available way to check this correlation can be provided by doing comparison with computed results issuing from a reduced kinetics scheme which describes with a good accuracy the major features of the hydroxyl radical chemistry [21]. The flame has been modeled as one-dimensional using CHEMKIN II [22] and PREMIX computer codes [23] and the following initial experimental characteristics:  $X_{\text{CH}_3\text{OH}}^0 = 0.125$ ,  $X_{\text{O}_2}^0 = 0.175$ ,  $X_{\text{N}_2}^0 = 0.70$ ; equivalence ratio = 1.08; inlet mass flow rate =  $3.15 \times 10^{-3} \text{ g cm}^{-2} \text{ s}^{-1}$ ; pressure = 0.052 atm; initial temperature = 298 K. The experimental corrected temperature profiles, determined without and with the presence of the quartz probe, have been successively introduced as input parameter in order to avoid the resolution of the energy equation. Such a procedure makes it possible to account, in each case, for heat losses from the flame.

In Fig. 5, modeled OH mole fraction profiles (lines) are compared with those experimentally measured by LIF (symbols) in the presence or not of the probe. Comparison does not require any scaling factor, as absorption technique allows absolute OH calibration. Agreement between experiments and model is very satisfying, except in the flame front region where the calculated OH peak value is 20% under the measured value, just at the estimated confidence limit for the absorption measurement. The model predicts with a very good accuracy both the experimental downstream shift of the reaction zone and the OH concentration decrease when the probe is introduced in the flame. According to these observations, we can consider that (1) probe presence does not alter significantly the OH reaction pathway, (2) as temperature profile is the unique input parameter modified for probe effect modeling, the cooling effect due to the presence of the probe, determined and measured by LIF, is responsible for OH profile change and (3) the probe volume location is well taken into account in our experiments according to our experimental procedure [6].

Importance of temperature correction is also illustrated in Fig. 5, where an OH profile, calculated from a not-corrected temperature profile is reported in case of probe presence. Temperatures were deduced from LIF intensities normalized by the laser intensities measured by a photodiode located in front of the burner. OH gradient position is well predicted, but sharper, and a 20% surestimation of OH mole fraction appears in the burnt gases, which presumably can alter flame kinetics understanding.

## 4 Conclusion

In order to improve temperature measurements in flames by LIF, we have developed a theoretical method which takes into account LIF signal attenuation due to both absorption of the laser and trapping of the fluorescence. Computed correction procedure is valid in case of flat flames within optical thin limit. Temperature corrections

vary linearly with OH concentration and depend on flame temperature. They can be extrapolated in a large range of flame conditions or burner diameters. In case of OH (0-0) excitation, corrections can be greater than the temperature statistical error (30 K) but are reliable. They are found about four times lower in case of (1-0) excitation as long as VET is limited. If that is not the case, accurate preliminary study of VET is required in the flame.

Corrected LIF method has been used to determine the temperature of the actual probe sampled volume. Following an experimental procedure already described [6], both OH and temperature profiles of the effective probe sampled volume are measured in a 40 Torr methanol/air flame and are compared with the unperturbed profiles. This study clearly points out, for the first time by LIF, a cooling effect reaching 100 K in the burnt gases. Accuracy of corrected temperature measurements and joint measurements of OH and temperature at the same location have been a good check of evaluating the correlation between the thermal effect and the observed OH profile change induced by the probe. According to model predictions, issuing from a reduced chemical mechanism, this correlation is shown important for the highly temperature-dependent OH species. The LIF method, developed in this paper, should lead to a great improvement of temperature measurement in flames, in the context of coupling with probe sampling techniques.

*Acknowledgements.* The authors would like to thank Prof. M.J. Cottreau (University of Rouen, France) for helpful discussions about LIF results interpretation.

## References

1. J.C. Biordi, C.P. Lazzara, J.F. Papp: *Combust. Flame* **23**, 73-82 (1974)
2. J.F. Pauwels, M. Carlier, P. Devolder and L.R. Sochet: *Combust. Sci. Technol.* **64**, 97 (1989)
3. K.J. Rensberger, J.B. Jeffries, R.A. Copeland, K. Kohse-Höinghaus, M.L. Wise, D.R. Crosley: *Appl. Opt.* **28**, 3556-3566 (1989)
4. R.J. Cattolica, Th. Mataga: *Chem. Phys. Lett.* **182**, 623-631 (1991)
5. K. Kohse-Höinghaus, J.B. Jeffries, R.A. Copeland, G.P. Smith, D.R. Crosley: In *Proc. 22nd Symp. (Int'l) on Combustion* (The Combustion Institute, Pittsburgh, PA 1988) pp. 1857-1866
6. P. Desgroux, L. Gasnot, J.F. Pauwels, L.R. Sochet: *Combust. Sci. Technol.* **100**, 379 (1994)
7. A.C. Eckbreth: In *Laser Diagnostics for Combustion Temperature and Species*, ed. by A. K. Gupta, D. G. Lilley (Abacus, Turnbridge Wells, MA 1988)
8. R.J. Cattolica: Sandia National Lab. Rep. SAND79-8717 (1979)
9. G.P. Smith, D.R. Crosley: *Appl. Opt.* **22**, 1428-1430 (1983)
10. R.A. Copeland, M.L. Wise, D.R. Crosley: *J. Phys. Chem.* **92**, 5710 (1988)
11. C.B. Cleveland, J.R. Wiesenfeld: *Chem. Phys. Lett.* **144**, 479-485 (1988)
12. K. Kohse-Höinghaus, U. Meier, B. Attal-Tretout: *Appl. Opt.* **29**, 1560-1569 (1990)
13. H.M. Hertz, M. Aldén: *Appl. Phys. B.* **42**, 97-102 (1987)
14. D.E. Heard, J.B. Jeffries, G.P. Smith, D.R. Crosley: *Combust. Flame* **88**, 137-148 (1992)
15. D. Stepowski, A. Garo: *Appl. Opt.* **24**, 2478-2480 (1985)
16. I.L. Chidsley, D.R. Crosley: *J. Quant. Spectrosc. Radiat. Transfer* **15**, 187-199 (1980)
17. P. Desgroux, E. Domingues, M.J. Cottreau: *Appl. Opt.* **31**, 2831-2838 (1992)
18. O.I. Smith, D.W. Chandler: *Combust. Flame* **63**, 19-29 (1986)
19. D. Stepowski, D. Puechberty, M.J. Cottreau: In *18th Symp. (Int'l) on Combustion* (The Combustion Institute, Pittsburgh, PA 1981) pp. 1567-1573
20. R.J. Cattolica, S. Yoon, E.L. Knuth: *Combust. Sci. Technol.* **28**, 225 (1982)
21. J.F. Pauwels, M. Carlier, P. Devolder, L.R. Sochet: *Combust. Flame* **82**, 163 (1990)
22. R.J. Kee, F.M. Rupley, J.A. Miller: Sandia National Lab. Rep. SAND89-8009 (1989)
23. R.J. Kee, J.F. Gear, M.D. Smooke, J.A. Miller: Sandia National Lab. Rep. SAND85-8240 (1985)